Supplementary Information for

Dynamic regimes of electrified liquid filaments

Tiantian Kong[1,2,*], Howard A. Stone[3,*], Liqiu Wang[2,4], Ho Cheung Shum[2,5,*]

[1]*Guangdong Key Laboratory for Biomedical Measurements and Ultrasound Imaging, Department of Biomedical Engineering, School of Medicine, Shenzhen University, Shenzhen, China*

[2]*Department of Mechanical Engineering, University of Hong Kong, Hong Kong*

[3] *Department of Mechanical and Aerospace Engineering, Princeton University, Princeton, New Jersey, USA*

[4]*HKU-Zhejiang Institute of Research and Innovation (HKU-ZIRI), Hangzhou, Zhejiang, China*

[5]*HKU-Shenzhen Institute of Research and Innovation (HKU-SIRI), Shenzhen, Guangdong, China*

*Correspondence and requests for materials should be addressed to T.T.K, H.A.S. and H.C.S.
Email: ttkong@szu.edu.cn; hastone@princeton.edu; ashum@hku.hk

This PDF file includes:

1) Supplementary text Section I-VI
2) Table S1
3) Figs S1 to S4
4) Caption for Movie S1
5) References for SI reference citations

www.pnas.org/cgi/doi/10.1073/pnas.1801053115

Supplementary Information Text

Section I. The minimum flow rate for jetting

In the absence of an electric field, a liquid jet tends to break up into droplets due to the Rayleigh-Plateau instability. The fate of the dispensed jet over a distance of L depends on the relative importance of two timescales: the dispensing time from the nozzle to the substrate, $\tau_f \sim L/U$, where U is the characteristic average velocity of dispensing, and the breakup timescale for viscous liquids $\tau_\mu \sim 2\mu a_0/\gamma$, where μ, γ and a_0 denote the viscosity, surface tension of the liquid, and the nozzle radius, respectively (1). The viscous timescale is employed when the Ohnesorge number, $Oh= \mu^2/\rho\gamma a_0$, denoting the viscous effects relative to the surface tension and inertial effects, is larger than 1. Thus, a continuous jet is dispensed, provided $\tau_f < \tau_\mu$ which is equivalent to the capillary number $Ca = \mu U/\gamma > L/2a_0$; otherwise, a train of drops is observed.

For a given liquid, at a fixed separation and nozzle size, increasing the flow rate triggers the transition from dripping to jetting. Above a critical flow rate $Q_c = \pi\gamma a_0 L/2\mu$, which is proportional to the capillary velocity γ/μ, a pinned liquid jet with a "bridge" shape forms (2).

Section II. The electrostatics of the leaky dielectric liquid jet

The liquid for the jet is characterized by both dielectric and conductive electrical responses; thus it is referred to as a leaky dielectric (3). The permittivity of the inner jet, ε_i, varies from 1.68×10^{-10} F/m to 3.71×10^{-10} F/m, depending on the liquids we used (*Materials and Methods*). The permittivity of the surrounding outer liquid, ε_o, is 8.85×10^{-12} F/m and 1.77×10^{-11} F/m for ambient air and silicone oil respectively. The electrical conductivity of the inner jet, K_i, ranges from 10^{-8} S/m to 10^{-4} S/m, which are at least four orders of magnitude higher than that of the surrounding dielectric liquids, $K_o=10^{-12}$ S/m (4). The charge per unit area at the interface is $\sigma = \varepsilon_o E_o^n - \varepsilon_i E_i^n$, where the superscript n denotes the normal component of the electric field, and the subscripts, i and o, denote the inner and outer liquids respectively.

Based on charge conservation $K_oE_o^n = K_iE_i^n$, we then have $\sigma = (\varepsilon_o - \varepsilon_i \frac{K_o}{K_i})E_o^n \sim \varepsilon_o E_o^n$ (5-7), provided $K_o \ll K_i$.

Assuming a slender shape where the jet radius a is much smaller than its length L, the normal electric stress across the jet interface can be approximated as $\frac{1}{2}(\varepsilon_i - \varepsilon_o)E^2 \approx \frac{1}{2}\varepsilon_i E^2$ (8-9), since ε_i is at least one order of magnitude larger than ε_o. Thus, the electrocapillary number describing the ratio of the electric stress to the capillary stress can be estimated as $\mathcal{E}_c = \varepsilon_i E^2 a_0/\gamma$, where a_0 is the nozzle radius.

Section III. The derivation of the governing equation of an axisymmetric liquid bridge in an axial electric field

Applying Newton's second law of motion to an element of the liquid bridge, as shown in Fig. 1*a*, the axial balance is among viscous, surface tension, gravitational, tangential electrostatic stress and inertial effects (10-14). At steady state, we have

$$\frac{3\mu}{a^2}(a^2v')' - (\frac{\gamma}{a})' + \rho g + \frac{\sigma E_t}{a} = \rho v v' \qquad \text{S1}$$

where $a(x)$ denotes the local radius and $v(x)$ is the velocity along the axial direction x; ρ, γ, σ and g are density, surface tension, surface charge density of the liquid, and gravitational acceleration respectively; $()'$ denotes "$d()/dx$", $\sigma E_t \cong \sigma E$ is the tangential electric stress along the liquid interface (3, 8, 15).

Since the flow rate is kept a constant, and $Q = \pi v a^2$,

$$2aa'v + a^2v' = 0$$

Taking

$$v' = -\frac{2Q}{\pi a^3}a', \quad v'' = (-\frac{2Q}{\pi})(-3\frac{(a')^2}{a^4} + \frac{a''}{a^3}) \qquad \text{S2}$$

The Eq. **S1** becomes (10-13)

$$\frac{\gamma}{a^2}a' + \frac{6\mu Q}{\pi a^4}(3(a')^2 - aa'') + \frac{2a'}{a}\left(-\frac{6\mu Q}{\pi a^3}a'\right) + \rho g + \frac{\sigma E_t}{a} = -\frac{2\rho Q^2}{\pi^2 a^5}a' \qquad \text{S3}$$

$$\frac{\gamma}{a^2}a' + \frac{6\mu Q}{\pi a^4}((a')^2 - aa'') + \rho g + \frac{\sigma E_t}{a} = -\frac{2\rho Q^2}{\pi^2 a^5}a' \qquad \text{S4}$$

The left-hand side terms correspond to pressure, viscous effects, gravitational body forces and tangential electric stress respectively, and the right-hand term is the inertial term.

If the pressure (governed by surface tension), gravitational and inertial terms are neglected (10), Eq. **S4** becomes

$$\frac{6\mu Q}{\pi a^4}((a')^2 - aa'') + \frac{\sigma E_t}{a} = 0 \qquad \text{S5}$$

We non-dimensionalize the above equation as follows:

$$x^* = \frac{x}{a_0} \quad \text{and} \quad a^* = \frac{a}{a_0} \qquad \text{S6}$$

The corresponding boundary conditions are $a/a_0 = 1$ at $x = 0$ and $a/a_0 = \infty$ at $x = L/a_0$, where L/a_0 is the dimensionless distance from the nozzle to the stagnation surface.

Now we drop the notation * and then we have

$$(a')^2 - aa'' + \frac{a^3}{{K_1}^2} = 0, \qquad \text{S7}$$

where ${K_1}^2 = \frac{6\mu Q}{\pi\sigma E_t a_0^3} \sim \frac{6\mu QL}{\pi\varepsilon_o E^2 a_0^4}$, since $\sigma E_t \sim \varepsilon_o E_n E_t \sim \varepsilon_o \frac{a_0}{L} E^2$ (8)

Let $a' = da/dx = A(a)$, then

$$a'' = \frac{d}{dx}\left(\frac{da}{dx}\right) = \frac{da}{dx}\frac{d}{da}\left(\frac{da}{dx}\right) = A\frac{dA}{da} \qquad \text{S8}$$

Thus, Eq. **S7** becomes

$$2A^2 - a\frac{d(A^2)}{da} = -\frac{2a^3}{K_1^2} \qquad \text{S9}$$

$$-\frac{2A^2}{a^3} + \frac{1}{a^2}\frac{d(A^2)}{da} = \frac{2}{K_1^2} \qquad \text{S10}$$

or

$$\frac{d}{da}\left(\frac{A^2}{a^2}\right) = \frac{2}{K_1^2} \qquad \text{S11}$$

so that

$$\frac{A^2}{a^2} = \frac{2}{K_1^2}a + c_1 \qquad \text{S12}$$

Now,

(1) if $c_1 = 0$, $\quad a' = \frac{da}{dx} = \sqrt{\frac{2a^3}{K_1^2}}, \quad d\left(a^{-\frac{1}{2}}\right) = \pm\frac{1}{\sqrt{2}K_1}x + c_2,$

and we find

$$a = \left(\pm\frac{1}{\sqrt{2}K_1}x + c_2\right)^{-2} \qquad \text{S13}$$

From the boundary conditions, we can deduce $c_2 = 1$, and $\pm\frac{1}{\sqrt{2}K_1}\frac{L}{a_0} + 1 = 0$, thus

$$a = \left(1 - \frac{1}{\sqrt{2}K_1}x\right)^{-2}, \qquad \text{at } \frac{L}{a_0} = \sqrt{2}K_1 \ \text{ which is } \beta = \frac{1}{\sqrt{2}K_1}\frac{L}{a_0} = 1 \qquad \text{S14}$$

Alternatively,

(2) if $c_1 \neq 0$, $\quad \frac{a'}{a} = \pm\sqrt{\frac{2a}{K_1^2} + c_1}, \qquad \frac{da}{a\sqrt{a + c_1 K_1^2/2}} = \pm\frac{\sqrt{2}}{K_1}dx$,

For $c_1 > 0$, $\quad a = \dfrac{{K_1}^2 c_1/2}{sinh^2\left(\pm\frac{\sqrt{c_1}}{2}(x + c_2)\right)}$ S15

Let $c_3 = {K_1}^2 c_1/2, \quad c_4 = \frac{\sqrt{c_1}}{2}c_2$, then from the boundary conditions, we have

$$sinh^2(c_4) = c_3\ ; \quad \frac{sinhc_4}{\sqrt{2}K_1}\frac{L}{a_0} \pm c_4 = 0 \quad \text{which is} \quad \beta sinhc_4 \pm c_4 = 0 \qquad \text{S16}$$

This cannot be solved unless $\beta < 1$, suggesting $a_0 < a_{min}$, which is not consistent with the experimental observations.

For $c_1 < 0$,

$$a = \frac{{K_1}^2 c_1}{2}\left(\left(\tan\left(\pm\frac{\sqrt{c_1}}{2}x + d_1\right)\right)^2 + 1\right) \qquad \text{with } d_1 = \frac{\sqrt{c_1 K_1/2}}{2}c_2 \qquad \text{S17}$$

From the boundary conditions, we can deduce

$$\sqrt{\frac{1}{1 + (\tan d_1)^2}} = \cos d_1 = \sqrt{\frac{c_1 {K_1}^2}{2}}; \qquad \text{S18}$$

$$\frac{\sqrt{\frac{c_1 {K_1}^2}{2}}}{\sqrt{2}K_1}\frac{L}{a_0} + d_1 = \frac{\pi}{2} \quad \text{which is} \quad (\cos d_1)\,\beta + d_1 = \frac{\pi}{2} \qquad \text{S19}$$

The solution exists with $\beta > 1, L/a_0 > \sqrt{2}K_1$ and it is consistent with the experimental results.

Section IV. The scaling of $\cos^2 d_1$ and β

The minimum jet radius corresponds to the derivative of the solution $a' = 0$, thus we deduce the minimum jet radius $a_{min} = \cos^2 d_1$, where d_1 is the root of the Eq. **S18**. Based on our experimental parameters, the range of β is from 2 to 10 ($\beta > 1$). We find that $a_{min} \sim \cos^2 d_1 \sim \beta^{-2}$ (Fig. S3), leading to $a_{min}/a_0 \sim 2K_1^2 a_0^2 L^{-2}$ ($\beta > 1$).

Section V. The charge transport for coiling and whipping jets

The whipping instability occurs simultaneously with the transition of charge transport from conduction to convection. When the bridge is straight with a sufficiently large radius, the bulk current is purely by conduction and the bridge is stable against whipping (16). The measured total current I scaled by the estimated conduction current $I/I_{conduction}$ for a coiling jet, is close to 1, where $I_{conduction} = \pi E K a^2$, and K is the electrical conductivity of the liquid (Fig. S4) (6), suggesting the charges are conducted for coiling jets. For whipping jets, $I/I_{conduction}$ is much larger than 1.

Section VI. The enhanced stability of a liquid bridge at close separation between electrodes

One hypothesis for the enhanced stability against the whipping instability at small separation between electrodes is that the space charges neutralize partial charges at the jet surfaces, and the repulsion between surface charges is therefore suppressed (17). This mechanism is ruled out for our experiments, since the breakdown field strength of the surrounding dielectric liquid in our cases, silicone oil, is ~15.4 kV/mm (18), which is much higher than the field strength we applied, ~ 0.1 kV/mm. The field strength to trigger whipping in our experiments is also much lower, 0.9 kV/mm, in (17), since we operate in a liquid-liquid system with a lower interfacial tension than a liquid-air system. Therefore, the slow decrease in the neck radius of the liquid bridge a_{min} under a close separation L, leading to a slow increase in surface charge density $\sigma \sim \varepsilon_o E_n \sim \sqrt{2\gamma/\varepsilon_o a_{min}}$ (6), thus contributing to the stabilization against the whipping instability.

Table S1. The measured viscosities of various working liquids.

Composition of liquid	Viscosity (*Pa.s*)
Lecithin from soy bean	7.5
Glyercin	1.41
1 wt% water in glyercin	1.14
2 wt% water in glyercin	0.93
5 wt% water in glyercin	0.56

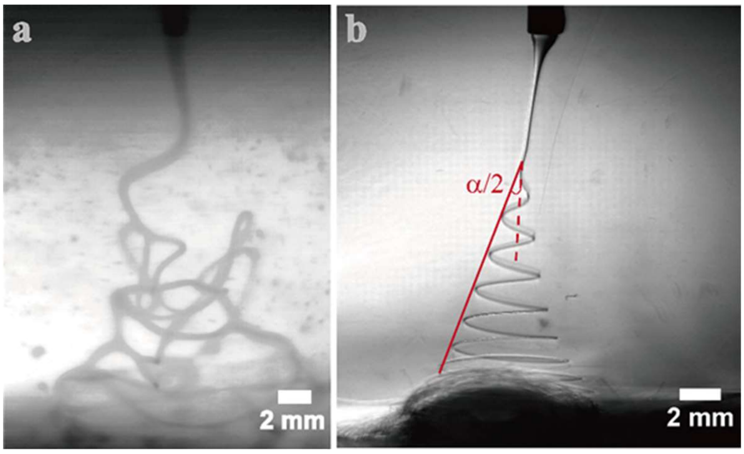

Fig. S1. Optical microscope images show the whipping structures of electrified liquid jets. a) A glycerin jet that whips chaotically in paraffin oil with 2% Span 80. b) A whipping lecithin jet forms a wave-like structure with a constant opening angle α in silicone oil of viscosity 10 mPa·s, similar to the structure observed in (19).

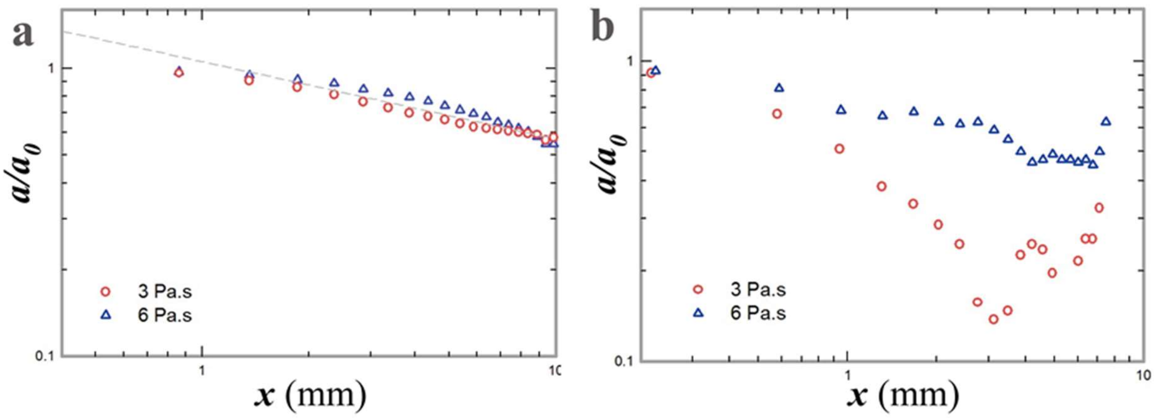

Fig. S2. Plot of the normalized jet radius a/a_0 against the axial distance x. a) Silicone oil jets (with viscosity of 3 Pa·s and 6 Pa·s) dispensed in air: separation *L*=0.5 *m*, *Q*=85 ml/hr. b) Silicone oil jets (with viscosity of 3 Pa·s and 6 Pa·s) dispensed in silicone oil of 20 mPa.s; separation *L*=0.014 m, *Q*=1 ml/hr. The nozzle size for the data in both plots is 0.92 mm.

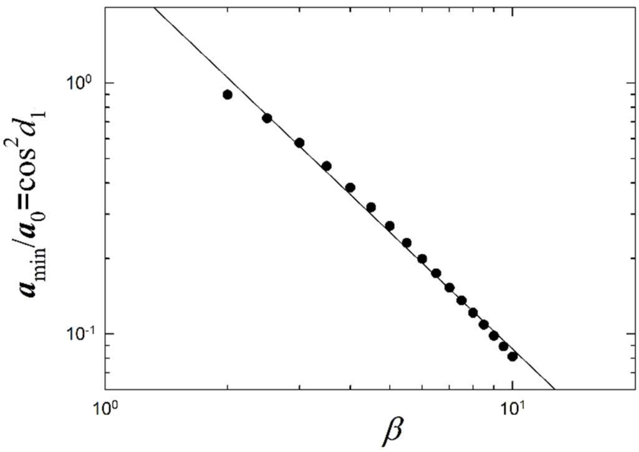

Fig. S3. A log-log plot of the experimental parameter $\beta = \frac{1}{\sqrt{2}K_1}\frac{L}{a_0}$ against the numerical value of $\cos^2 d_1$, where d_1 is the root of Eq. S18.The range of β is from 2 to 10, covering all of our experiments. All data points collapse onto a solid line representing a power-law fit with an exponent of -2, implying $\cos^2 d_1 \sim \beta^{-2}$.

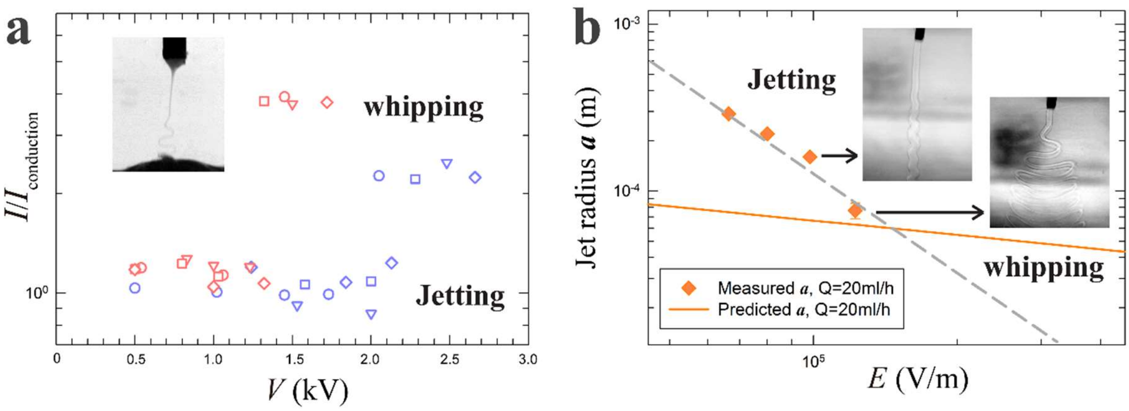

Fig. S4. a) Experimentally measured current I scaled with $I_{conduction}$ as a function of the applied voltage for different interfacial tensions: γ=2 mN/m (red) and γ=6.7 mN/m (blue). b) A plot of the measured a_{min} against the applied E. The dashed line indicates the scaling between a_{min} and E, $a_{min}{\sim}E^{-2}$; the solid line represents the $a{\sim}(2Q\sigma/EK)^{1/3}$ below which $I_{conduction} = \pi EKa^2$ is smaller than $I_{convection} = 2\sigma Q/a$ (10). Here Q=20 ml/h, Σ=4×10^{-5} S/m, γ=2 mN/m.

Movie S1. A high-speed video showing the dynamic behaviors "jetting", "coiling" and "whipping" of an electrified liquid filament, respectively. The applied voltage increases from 0 kV to 1.5 kV. A liquid filament of a solution of lecithin with a viscosity of μ=7.5 Pa.s is extruded from a nozzle with a radius of a_0=0.92 mm at a fixed flow rate Q=10 ml/h into a bath of silicone oil with a viscosity of μ=10 mPa·s.

Reference

1. Eggers J, Villermaux E (2008) Physics of liquid jets. *Reports Prog Phys* 71(3):36601.
2. Kong T, et al. (2016) Rapid mixing of viscous liquids by electrical coiling. *Sci Rep* 6:19606.
3. Saville DA (1997) Electrohydrodynamics: the Taylor-Melcher leaky dielectric model. *Annu Rev Fluid Mech* 29(1):27–64.
4. Sankaran S, Saville DA (1993) Experiments on the stability of a liquid bridge in an axial electric field. *Phys Fluids* 5(4):1081-1083.
5. Ganan-Calvo AM, Davila J, Barrero A (1997) Current and droplet size in the elctrospraying of liquids. scaling laws. *J Aerosol Sci* 28(2):249–275.
6. Gundabala VR, Vilanova N, Fernandez-Nieves A (2010) Current-voltage characteristic of electrospray processes in microfluidics. *Phys Rev Lett* 105(15):154503.
7. Fernández de la Mora J (2007) The fluid dynamics of taylor cones. *Annu Rev Fluid Mech* 39(1):217–243.
8. Stone HA, Lister JR, Brenner MP (1999) Drops with conical ends in electric and magnetic fields. *Proc R Soc A Math Phys Eng Sci* 455:329–347.
9. Hohman MM, Shin M, Rutledge GC, Brenner MP (2001) Electrospinning and electrically forced jets. I.Stability theory. *Phys Fluids* 13(8):2201–2220.
10. Cruickshank J, Munson B (1982) The viscous-gravity jet in stagnation flow. *J Fluids Eng* 104(3):360-362.
11. Matovich MA, Pearson JRA (1969) Spinning a molten threadline: steady-state isothermal viscous flows. *Ind Eng Chem Fundam* 8(3):512–520.
12. Pearson JRA, Matovich MA (1969) Spinning a molten threadline: stability. *Ind Eng Chem Fundam* 8(4):605–609.
13. Hohman MM, Shin M, Rutledge G, Brenner MP (2001) Electrospinning and electrically forced jets. II. Applications. *Phys Fluids* 13(8):2221–2236.
14. Higuera FJ (2006) Stationary viscosity-dominated electrified capillary jets. *J Fluid Mech* 558:143-152.
15. Sherwood JD (1988) Breakup of fluid droplets in electric and magnetic fields. *J Fluid Mech* 188(1):133-146.
16. Zhao Y, Bober DB, Chen CH (2011) Nonclogging resistive pulse sensing with electrohydrodynamic cone-jet bridges. *Phys Rev X* 1(2):021007.
17. Korkut S, Saville DA, Aksay IA (2008) Enhanced stability of electrohydrodynamic jets through gas ionization. *Phys Rev Lett* 100(3):034503.
18. Lide DR, et al. (2010) CRC Handbook of Chemistry and Physics. *CRC Press*.
19. Guerrero J, Rivero J, Gundabala VR, Perez-Saborid M, Fernandez-Nieves A (2014) Whipping of electrified liquid jets. *Proc Natl Acad Sci* 111(38):13763–13767.